

Effects of hydrostatic pressure on magnetostructural transitions and magnetocaloric properties in $(\text{MnNiSi})_{1-x}(\text{FeCoGe})_x$

Tapas Samanta,^{1,a)} Daniel L. Lepkowski,¹ Ahmad Us Saleheen,¹ Alok Shankar,¹ Joseph Prestigiacomo,¹ Igor Dubenko,² Abdiel Quetz,² Iain W. H. Oswald,³ Gregory T. McCandless,³ Julia Y. Chan,³ Philip W. Adams,¹ David P. Young,¹ Naushad Ali,² and Shane Stadler¹

¹Department of Physics and Astronomy, Louisiana State University, Baton Rouge, Louisiana 70803, USA

²Department of Physics, Southern Illinois University, Carbondale, Illinois 62901, USA

³Department of Chemistry, The University of Texas at Dallas, Richardson, Texas 75080, USA

(Received 21 January 2015; accepted 17 March 2015; published online 26 March 2015)

The isostructural alloying of two compounds with different magnetic and thermo-structural properties has resulted in a new system, $(\text{MnNiSi})_{1-x}(\text{FeCoGe})_x$, that exhibits large magnetocaloric effects with acute sensitivity to both compositional variation and applied hydrostatic pressure. The maximum isothermal entropy change reaches a value of $-\Delta S^{\max} = 143.7 \text{ J/kg K}$ for a field change of $\Delta B = 5 \text{ T}$ at atmospheric pressure. The first-order magnetostructural transition responsible for the entropy change shifts to lower temperature with applied hydrostatic pressure ($\sim -10 \text{ K/kbar}$) but maintains a large value of $-\Delta S^{\max}$. © 2015 AIP Publishing LLC.

[<http://dx.doi.org/10.1063/1.4916339>]

I. INTRODUCTION

In recent years, considerable attention has been devoted to studies of Mn-based MnTX ($T = \text{Co, Ni}$ and $X = \text{Ge, Si}$) systems due to their temperature-induced magnetostructural transitions (MSTs) that result in shape memory phenomena, giant magnetocaloric effects (MCEs), and volume anomalies near room temperature.^{1–9} Some also behave as strongly correlated electron systems in the proximity of a noncollinear ferromagnetic state.¹⁰ In particular, the coincidence of magnetic and structural transitions near room temperature, accomplished by properly tuning the stoichiometry and chemical composition, often results in large MCEs, making these systems of great interest in the field of magnetocalorics.

MnTX is a class of materials that exhibits different kinds of magnetic structures depending on composition, such as collinear ferromagnetic structures (in MnCoGe), spiral anti-ferromagnetic structures (in MnNiGe), noncollinear helical antiferromagnetic structures (e.g., CoMnSi), and so on. The above mentioned systems show second order magnetic transitions near room temperature. However, stoichiometric MnNiGe , MnCoGe , and CoMnSi systems undergo martensitic structural transitions from a low-temperature TiNiSi -type structure to a high-temperature hexagonal Ni_2In -type structure in the paramagnetic state.

Considerable attention has been given to the MnCoGe and MnNiGe -based systems in the context of magnetocaloric effects due to their closely spaced magnetic and structural transitions, and the potential to couple them near room temperature by changing the stoichiometry, chemical substitution, or by applying pressure. However, the MnNiSi compound undergoes a structural transition from a low-temperature orthorhombic TiNiSi -type structure to a

high-temperature hexagonal Ni_2In -type structure at an extremely high temperature of about 1200 K in the paramagnetic state, and undergoes a second-order ferromagnetic transition at $T_C = 662 \text{ K}$.^{11,12} It is important to tune the coupled transition (and therefore the operating temperature of the MCE) so that it occurs near room temperature, a feat that, in this case, could not be accomplished with a single-element substitution. As an alternative substitution strategy, MnNiSi was alloyed with isostructural FeCoGe (having a stable hexagonal Ni_2In -type structure and $T_C \sim 370 \text{ K}$ (Ref. 13)), which stabilized the hexagonal Ni_2In -type phase by sharply reducing the structural transition temperature from 1200 K in MnNiSi to less than 300 K in $(\text{MnNiSi})_{1-x}(\text{FeCoGe})_x$. A similar type of scheme was previously employed to position the MST near room temperature by substituting FeNiGe and MnFeGe in MnNiSi .^{4,14} Hexagonal FeCoGe was also selected for another reason: it exhibits a large saturation magnetization ($M_S \sim 2 \mu_B$).

A strong coupling of magnetic and structural degrees of freedom often results in large MCEs, as observed in many well-known magnetocaloric materials in the vicinity of a magnetostructural transition, and is accompanied by changes in crystal symmetry or volume. A large structural entropy change associated with a significant volume change due to the structural transition can enhance the total entropy change in MnTX systems in comparison to other well-known giant magnetocaloric materials. Pressure is a controllable external parameter that can affect the structural entropy change of a system and, as a result, a pressure-induced modification of magnetocaloric properties could be expected in some MnTX systems. Recent reports on hydrostatic-pressure studies also indicate the possibility of applying pressure to improve the magnetocaloric properties by demonstrating a large isothermal entropy change.^{14–16}

Here we report a system, $(\text{MnNiSi})_{1-x}(\text{FeCoGe})_x$, for which applied hydrostatic pressure, as well as minor

^{a)}Author to whom correspondence should be addressed. Electronic mail: tapas.sinp@gmail.com

variations of composition, shifts the temperature of the coupled MST responsible for the MCE. A large tunable MCE has been observed in this system over a wide temperature range spanning room temperature.

II. SAMPLE PREPARATION AND CHARACTERIZATION

Polycrystalline $(\text{MnNiSi})_{1-x}(\text{FeCoGe})_x$ ($x = 0.37, 0.38, 0.39$, and 0.40) samples were prepared by arc-melting the constituent elements of purity better than 99.9% in an ultra-high purity argon atmosphere. The samples were annealed under high vacuum for 3 days at 750°C followed by quenching in cold water. Temperature-dependent X-ray diffraction (XRD) measurements to determine the crystal structures of the samples were conducted on a Bruker D8 Advance diffractometer using a Cu K α_1 radiation source ($\lambda = 1.54060\text{\AA}$) equipped with a LYNXEYE XE detector. Rietveld refinement was used to determine unit cell volumes and phase fractions above and below the phase transition temperatures using TOPAS. A superconducting quantum interference device magnetometer (SQUID, Quantum Design MPMS) was used to measure the magnetization (M) of the $(\text{MnNiSi})_{1-x}(\text{FeCoGe})_x$ samples within the temperature interval of 10 – 400 K , and in applied magnetic fields (B) up to 5 T . Magnetic measurements under applied hydrostatic pressure (P) were performed in a commercial BeCu cylindrical pressure cell (Quantum Design). Daphne 7373 oil was used as the pressure transmitting medium. The value of the applied pressure was calibrated by measuring the shift of the superconducting transition temperature of Pb which was used as a reference manometer (Pb has a critical temperature $T_C \sim 7.19\text{ K}$ at ambient pressure).¹⁷

III. EXPERIMENTAL RESULTS AND DISCUSSION

The temperature dependent XRD patterns of $(\text{MnNiSi})_{1-x}(\text{FeCoGe})_x$ with $x = 0.40$ are shown in Fig. 1. The observed hexagonal Ni₂In-type crystal structure at 290 K indicates that the substitution of FeCoGe in

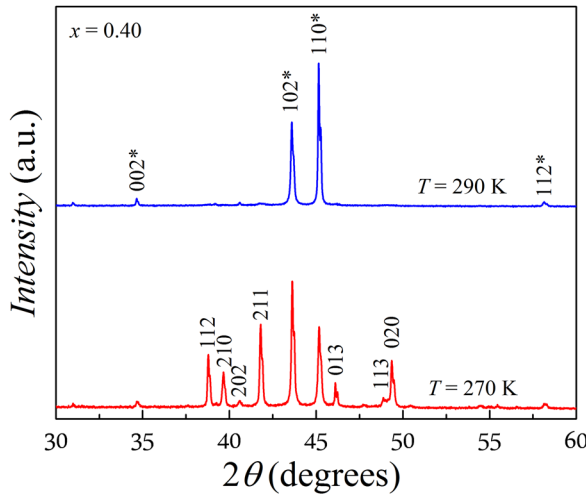


FIG. 1. XRD patterns for $x = 0.40$ measured at temperatures immediately above and below the magnetostructural transition. The Miller indices of the high-temperature hexagonal and low-temperature orthorhombic phases are designated with and without an asterisk (*), respectively.

$(\text{MnNiSi})_{1-x}(\text{FeCoGe})_x$ stabilizes the high-temperature hexagonal phase at a much lower temperature than that of the parent MnNiSi. An orthorhombic TiNiSi-type structure was detected at lower temperature (270 K) with traces of the hexagonal phase. These results indicate that the structural transition temperature decreases drastically by isostructurally alloying MnNiSi with FeCoGe.

The magnetization (M) as a function of temperature (T) data for $(\text{MnNiSi})_{1-x}(\text{FeCoGe})_x$, at ambient pressure as well as under the application of hydrostatic pressure, measured during heating and cooling in the presence of a 1 kOe magnetic field, are shown in Fig. 2. The sharp change in magnetization in the vicinity of the phase transition indicates a magnetic transition from a high-temperature paramagnetic (PM) state to a low-temperature ferromagnetic (FM) state. The thermal hysteresis between heating and cooling curves indicates that the magnetic and structural transitions coincide, leading to a single, first-order MST (at T_M) from a low-temperature orthorhombic FM state to a high-temperature hexagonal PM state. T_M shifts to lower temperature with increasing substitution of hexagonal FeCoGe while maintaining the coupled nature of the MST. The MST in the $(\text{MnNiSi})_{1-x}(\text{FeCoGe})_x$ compounds remains coupled for $0.37 \leq x \leq 0.40$, but spans a large temperature range of 235 to 355 K .

The application of hydrostatic pressure (P) has an effect that resembles that of increasing the concentration (x) of FeCoGe, shifting the MST to lower temperature by about -10 K per kbar of applied pressure ($dT_M/dP \sim -10\text{ K kbar}^{-1}$). In the orthorhombic crystal structure (Fig. 1), reducing the lattice parameter a_{ortho} distorts the geometry of the crystal structure in orthorhombic MnNiSi, resulting in a stabilization of the hexagonal structure.¹⁸ Since the orthorhombic lattice parameter a_{ortho} is equivalent to the hexagonal lattice parameter c_{hex} (i.e., $a_{\text{ortho}} = c_{\text{hex}}$), a decrease in the c/a ratio tends to stabilize the hexagonal structure. As a result, the structural transition temperature decreases with

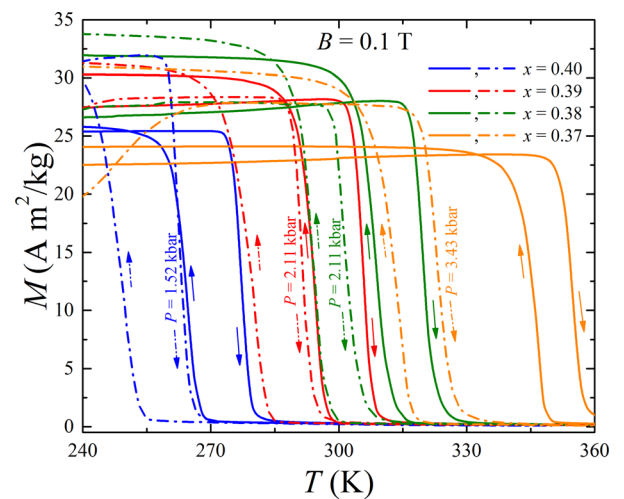


FIG. 2. Temperature dependence of the magnetization (M) in the presence of a 0.1 T magnetic field (B) during heating and cooling (direction indicated by arrows) for $(\text{MnNiSi})_{1-x}(\text{FeCoGe})_x$ as measured at ambient pressure (solid lines) and at different applied hydrostatic pressures (broken lines).

increasing x in response to the reduction of the c/a ratio induced by the substitution of FeCoGe in $(\text{MnNiSi})_{1-x}(\text{FeCoGe})_x$.

The shift in T_M with application of pressure is likely associated with a pressure-induced distortion of the orthorhombic lattice that increases the stability of the hexagonal phase. The similar response of T_M to both chemical substitution and applied hydrostatic pressure suggests the same physical origin of the temperature shift: chemical and physical pressures are closely related. From the pressure-induced shift in T_M , and the volume change through the MST as determined from temperature-dependent XRD, we estimated the equivalent average compressibility per unit substitution of FeCoGe to be approximately $7.93 \times 10^{-11} \text{ Pa}^{-1}$.

As estimated from magnetization isotherms (Fig. 3(a)) shows representative data for $x=0.40$) using the integrated Maxwell relation, $-\Delta S = \int_0^B \left(\frac{\partial M}{\partial T} \right)_B dB$, the material exhibits a large isothermal entropy change ($-\Delta S$) in the vicinity of the MST (Fig. 3(b)). Specifically, the $x=0.40$ compound has a $-\Delta S^{\max} = 143.7 \text{ J/kg K}$ for a field change of $\Delta B = 5 \text{ T}$, which is about 63% of theoretical limit $-\Delta S_{\text{th}}^{\max} = nR\ln(2J+1) = 228.4 \text{ J/kg K}$, where J is the total angular momentum of the magnetic ions, R is the universal gas constant, and n is the number of magnetic atoms per formula unit. The experimental results are summarized in Table I along with related parameters for other well-known giant magnetocaloric materials.

With the application of hydrostatic pressure, the peaks in the $-\Delta S(T)$ curves shift to lower temperatures at a rate of

about $dT_M/dP \sim -10 \text{ K/kbar}$, but the MCE remains robust over the temperature ranges shown (Fig. 3(b)). Since the large MCE is preserved in $(\text{MnNiSi})_{1-x}(\text{FeCoGe})_x$ as the MST shifts in temperature with applied pressure, an improvement of the effective “relative cooling power (RCP)” of the material can be realized. The RCP, which is the measure of the amount of heat transfer between the cold and hot reservoirs in an ideal refrigeration cycle, is defined as $\text{RCP} = |-\Delta S^{\max} \times \delta T_{\text{FWHM}}|$, where δT_{FWHM} is the full-width at half-maximum of the $-\Delta S$ vs. T plot. Therefore a good magnetic refrigerant material, i.e., one having a large RCP, requires not only a large value of $-\Delta S^{\max}$ but also a wide $-\Delta S(T)$ curve. Most other well-known giant MCE materials undergo first-order transitions, resulting in large values of $-\Delta S^{\max}$, but occur over a narrow temperature range, making them impractical for applications in most instances. One way to overcome this problem is to form composites of multiple first-order materials with MCEs in different temperature ranges, increasing the effective value of δT_{FWHM} , but decreasing the average $-\Delta S^{\max}$ (as normalized by the total mass of material). However, a more effective strategy could be to take advantage of the sensitivity of the transition temperature to applied hydrostatic pressure ($\sim 10 \text{ K/kbar}$). This is about 2 times higher than MnNiGe (-5.4 K/kbar).²⁶

In a theoretical work, it has been suggested that the effective refrigeration capacity of a material undergoing a first-order magnetic phase transition can be improved by applying hydrostatic pressure while simultaneously varying the applied magnetic field.²⁷ In essence, this means that the

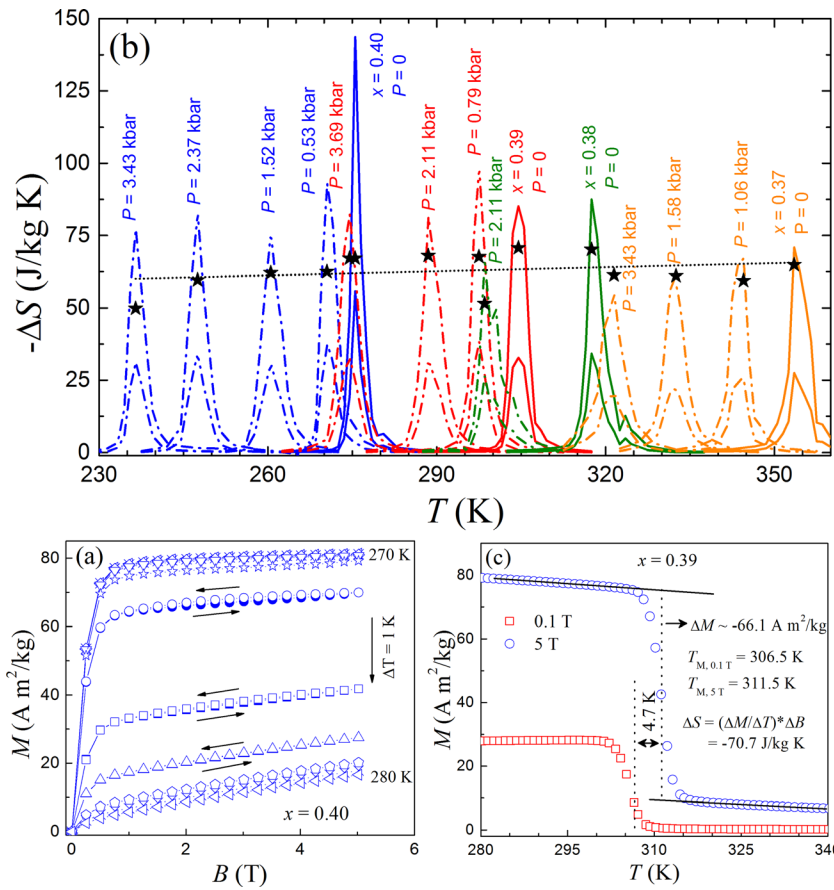


FIG. 3. (a) The isothermal magnetization curves for $x=0.40$. The arrows indicate the direction of the field sweep. (b) The isothermal entropy change ($-\Delta S$) as a function of temperature were estimated using a Maxwell relation for magnetic field changes of $\Delta B = 5 \text{ T}$ (upper curves) and 2 T (lower curves), measured at ambient pressure (solid lines) and at different applied hydrostatic pressures (broken lines). The “star” symbols inside each $-\Delta S(T)$ curve represents the corresponding total entropy change estimated by employing the Clausius-Clapeyron equation for $\Delta B = 5 \text{ T}$. A linear fit of these values, intended as a guide to the eye, is indicated by a black dotted line. (c) Heating thermomagnetization curves for applied fields $B = 0.1$ and 5 T used to estimate the value of $-\Delta S$ for $x=0.39$ using the Clausius-Clapeyron equation.

TABLE I. Transition temperatures (T_C or T_M), and reported $-\Delta S^{\max}$ for materials exhibiting giant MCE, including $(\text{MnNiSi})_{1-x}(\text{FeCoGe})_x$ (present work), for a field variation of 5 T near room temperature.

Material	T_C or T_M (K)	$-\Delta S^{\max}$ (J/kg K)	References
Gd	294	10.2	¹⁹
$(\text{MnNiSi})_{1-x}(\text{FeCoGe})_x$			Present work
$x = 0.40$	276	143.7	
$x = 0.39$	305	85.2	
$x = 0.38$	318	87.5	
$(\text{NiMnSi})_{0.56}(\text{FeNiGe})_{0.44}$	292	11.5 for $\Delta B = 1$ T	⁴
$\text{Mn}_{1-x}\text{Cu}_x\text{CoGe}$			³
$x = 0.08$	321	53.3	
$x = 0.085$	304	52.5	
$x = 0.09$	289	41.2	
$x = 0.095$	275	34.8	
$x = 0.1$	249	36.4	
MnCoGeB_x			²
$x = 0.01$	304	14.6	
$x = 0.02$	287	47.3	
$x = 0.03$	275	37.7	
$\text{Mn}_{1-x}\text{Cr}_x\text{CoGe}$			⁷
$x = 0.04$	322	28.5	
$x = 0.11$	292	27.7	
$x = 0.18$	274	15.6	
$\text{Mn}_{1-x}\text{V}_x\text{CoGe}$			⁸
$x = 0.01$	322	8.7 for $\Delta B = 1.2$ T	
$x = 0.02$	298	9.5	
$x = 0.03$	270	3.4	
$\text{MnCo}_{0.95}\text{Ge}_{1.14}$	331	6.4 for $\Delta B = 1$ T	⁹
$\text{Gd}_5\text{Si}_2\text{Ge}_2$	272	36.4	²⁰
MnAs	318	30	²¹
$\text{MnFeP}_{0.45}\text{As}_{0.55}$	305	18	²²
$\text{La}(\text{Fe}_{0.88}\text{Si}_{0.12})_{13}\text{H}_1$	274	23	²³
$\text{Ni}_{55.2}\text{Mn}_{18.6}\text{Ga}_{26.2}$	320	20.4	²⁴
$\text{Ni}_2\text{Mn}_{1-x}\text{Cu}_x\text{Ga}$			²⁵
$x = 0.25$	318	64	
$x = 0.26$	309	42	

effective width of $-\Delta S(T)$ increases by an amount equal to the temperature shift in the $-\Delta S(T)$ peak with pressure. Therefore, together with the magnetic field, the observed pressure-induced shift in the MST may facilitate an increase in the effective refrigeration capacity in this system. If this pressure-field operation were applied to the sample with $x = 0.39$, the effective RCP would be enhanced by a factor of almost 15 relative to the ambient-pressure value ($\Delta P = 3.69$ kbar and $\Delta B = 5$ T). Interestingly, in this case, the effective temperature range spans room temperature through the freezing point of water (for $P = 0$ and $P = 3.69$ kbar, respectively), which may be ideal for certain cooling applications. Two things should be noted here. First, strictly defined, this is not the barocaloric effect (although this system may exhibit the barocaloric properties). Second, this so-called enhanced effective RCP has not been measured experimentally.

The structural entropy change ($-\Delta S_{\text{st}}$) associated with the volume change ΔV has been estimated (for $x = 0.40$) by employing the Clausius-Clapeyron equation, $\Delta S_{\text{st}} = -\Delta V \left(\frac{dT_M}{dP} \right)^{-1}$. The relative volume change $\frac{\Delta V}{V} \sim 2.85\%$

was determined from temperature-dependent XRD measurements made just above and below the MST (Fig. 2). The corresponding structural entropy change is $-\Delta S_{\text{st}} = 38.7$ J/kg K, which is about one-fourth of the total entropy change.

The Clausius-Clapeyron equation is considered to be more reliable than the Maxwell relation for calculating the entropy change near first-order transitions. Applying the Clausius-Clapeyron equation following Ref. 28, $[\frac{\Delta S}{\Delta M}] = \frac{dB}{dT} \approx \Delta S = (\Delta M / \Delta T) \Delta B$, for $x = 0.39$ (Fig. 3(c)) we obtain $-\Delta S^{\max} \sim 70.7$ J/kg K ($\Delta B = 5$ T) compared to 143.7 J/kg K using Maxwell relation. Representative data for one sample ($x = 0.39$) used to estimate $-\Delta S^{\max}$ using the Clausius-Clapeyron equation are shown in Fig. 3(c). Interestingly, the values of $-\Delta S^{\max}$ as estimated employing the Clausius-Clapeyron equation varies only moderately with composition as well as applied pressure. These values are comparable to those of other well-known MCE materials.

IV. SUMMARY

We have shown that combining two isostructural compounds with different magnetic and thermo-structural properties can result in new systems that possess magnetocaloric transitions with acute sensitivity to applied pressure and compositional variation. The magnetic compound, $(\text{MnNiSi})_{1-x}(\text{FeCoGe})_x$, represents a new class of room-temperature magnetocaloric materials that exhibits large, tunable magnetocaloric effects, and fit many criteria for magnetocaloric materials sought for devices, including: (i) negligible magnetic hysteresis losses; (ii) composed of non-toxic, abundant materials; and (iii) straightforward and repeatable synthesis processes. The characteristic that makes these new materials promising, however, is their sensitive response to applied hydrostatic pressure, which provides a means to optimize the magnetocaloric effect at any temperature within its active range.

ACKNOWLEDGMENTS

Work at Louisiana State University (S. Stadler) was supported by the U.S. Department of Energy (DOE), Office of Science, Basic Energy Sciences (BES) under Award No. DE-FG02-13ER46946, and heat capacity measurements were carried out at LSU by P. W. Adams who is supported by DOE, Office of Science, BES under Award No. DE-FG02-07ER46420. Work at Southern Illinois University was supported by DOE, Office of Science, BES under Award No. DE-FG02-06ER46291. D. P. Young fabricated samples and acknowledges support from the NSF through DMR Grant No. 1306392. J. Y. Chan acknowledges DMR-1360863 for support of X-ray measurements.

¹E. Liu, W. Wang, L. Feng, W. Zhu, G. Li, J. Chen, H. Zhang, G. Wu, C. Jiang, H. Xu, and F. de Boer, *Nature Commun.* **3**, 873 (2012).

²N. T. Trung, L. Zhang, L. Caron, K. H. J. Buschow, and E. Brück, *Appl. Phys. Lett.* **96**, 172504 (2010).

³T. Samanta, I. Dubenko, A. Quetz, S. Stadler, and N. Ali, *Appl. Phys. Lett.* **101**, 242405 (2012).

⁴C. L. Zhang, D. H. Wang, Z. D. Han, B. Qian, H. F. Shi, C. Zhu, J. Chen, and T. Z. Wang, *Appl. Phys. Lett.* **103**, 132411 (2013).

⁵T. Samanta, I. Dubenko, A. Quetz, S. Temple, S. Stadler, and N. Ali, *Appl. Phys. Lett.* **100**, 052404 (2012).

- ⁶E. K. Liu, W. Zhu, L. Feng, J. L. Chen, W. H. Wang, G. H. Wu, H. Y. Liu, F. B. Meng, H. Z. Luo, and Y. X. Li, *EPL* **91**, 17003 (2010).
- ⁷N. T. Trung, V. Biharie, L. Zhang, L. Caron, K. H. J. Buschow, and E. Brück, *Appl. Phys. Lett.* **96**, 162507 (2010).
- ⁸S. C. Ma, Y. X. Zheng, H. C. Xuan, L. J. Shen, Q. Q. Cao, D. H. Wang, Z. C. Zhong, and Y. W. Du, *J. Magn. Magn. Mater.* **324**, 135 (2012).
- ⁹Y. K. Fang, C. C. Yeh, C. W. Chang, W. C. Chang, M. G. Zhu, and W. Li, *Scr. Mater.* **57**, 453 (2007).
- ¹⁰T. Samanta, I. Dubenko, A. Quetz, J. Prestigiacomo, P. W. Adams, S. Stadler, and N. Ali, *Appl. Phys. Lett.* **103**, 042408 (2013).
- ¹¹V. Johnson, *Inorg. Chem.* **14**, 1117–1120 (1975).
- ¹²W. Bażela, A. Szytuła, J. Todorović, and A. Zieba, *Phys. Status Solidi A* **64**, 367 (1981).
- ¹³A. Szytuła, A. T. Pędziwiatr, Z. Tomkowicz, and W. Bażela, *J. Magn. Magn. Mater.* **25**, 176–186 (1981).
- ¹⁴T. Samanta, D. L. Lepkowski, A. Us Saleheen, A. Shankar, J. Prestigiacomo, I. Dubenko, A. Quetz, I. W. H. Oswald, G. T. McCandless, J. Y. Chan, P. W. Adams, D. P. Young, N. Ali, and S. Stadler, *Phys. Rev. B* **91**, 020401(R) (2015).
- ¹⁵L. Mañosa, D. González-Alonso, A. Planes, E. Bonnot, M. Barrio, J.-L. Tamarit, S. Aksoy, and M. Acet, *Nat. Mater.* **9**, 478 (2010).
- ¹⁶D. Matsunami, A. Fujita, K. Takenaka, and M. Kano, *Nat. Mater.* **14**, 73 (2015).
- ¹⁷A. Eiling and J. S. Schilling, *J. Phys. F* **11**, 623 (1981).
- ¹⁸G. A. Landrum, R. Hoffman, J. Evers, and H. Boysen, *Inorg. Chem.* **37**, 5754 (1998).
- ¹⁹K. A. Gschneidner, Jr., V. K. Pecharsky, and A. O. Tsokol, *Rep. Prog. Phys.* **68**, 1479 (2005).
- ²⁰V. K. Pecharsky and K. A. Gschneidner, Jr., *Phys. Rev. Lett.* **78**, 4494 (1997).
- ²¹H. Wada and Y. Tanabe, *Appl. Phys. Lett.* **79**, 3302 (2001).
- ²²O. Tegus, E. Brück, K. H. J. Buschow, and F. R. de Boer, *Nature (London)* **415**, 150 (2002).
- ²³A. Fujita, S. Fujieda, Y. Hasegawa, and K. Fukamichi, *Phys. Rev. B* **67**, 104416 (2003).
- ²⁴X. Zhou, W. Li, H. P. Kunkel, and G. Williams, *J. Phys.: Condens. Matter* **16**, L39 (2004).
- ²⁵S. Stadler, M. Khan, J. Mitchell, N. Ali, A. M. Gomes, I. Dubenko, A. Y. Takeuchi, and A. P. Guimarães, *Appl. Phys. Lett.* **88**, 192511 (2006).
- ²⁶S. Anzai and K. Ozawa, *Phys. Rev. B* **18**, 2173 (1978).
- ²⁷N. A. Oliveira, *Appl. Phys. Lett.* **90**, 052501 (2007).
- ²⁸R. Kainuma, Y. Imano, W. Ito *et al.*, *Nature* **439**, 957 (2006).



School of Natural Sciences and Mathematics

Effects of Hydrostatic Pressure on Magnetostructural Transitions and Magnetocaloric Properties in $(MnNiSi)_{1-x} (FeCoGe)_x$

©2015 AIP Publishing LLC. This article may be downloaded for personal use only. Any other use requires prior permission of the author and the American Institute of Physics.

Citation:

Samanta, Tapas, Daniel L. Lepkowski, Ahmad Us Saleheen, Alok Shankar, et al. 2015. "Effects of hydrostatic pressure on magnetostructural transitions and magnetocaloric properties in $(MnNiSi)_{1-x} (FeCoGe)_x$." Journal of Applied Physics 117(12): doi:10.1063/1.4916339.

This document is being made freely available by the Eugene McDermott Library of The University of Texas at Dallas. All rights are reserved under United States copyright law unless specified otherwise,